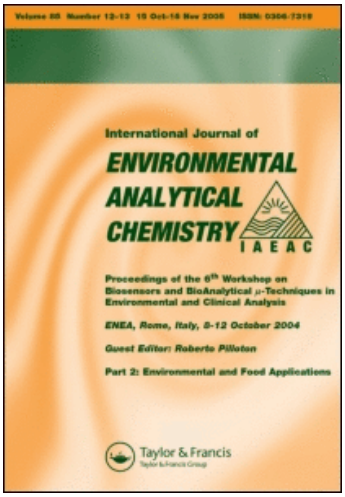

International Journal of Environmental Analytical Chemistry
Publication details, including instructions for authors and subscription information:
http://www.informaworld.com/smpp/title~content=t713640455

Signal enhancement of protein chips using 3D-materials for immobilization

Claudia Preininger[a]; Ursula Sauer[a]; Stefan Obersriebnig[a]; Max Trombitas[a]
[a] ARC Seibersdorf Research GmbH, Department of Bioresources, 2444 Seibersdorf, Austria

To cite this Article Preininger, Claudia , Sauer, Ursula , Obersriebnig, Stefan and Trombitas, Max(2005) 'Signal enhancement of protein chips using 3D-materials for immobilization', International Journal of Environmental Analytical Chemistry, 85: 9, 645 — 654
To link to this Article: DOI: 10.1080/03067310500154775
URL: http://dx.doi.org/10.1080/03067310500154775

Intern. J. Environ. Anal. Chem.
Vol. 85, Nos. 9–11, 10 August–15 September 2005, 645–654

Taylor & Francis
Taylor & Francis Group

Signal enhancement of protein chips using 3D-materials for immobilization

CLAUDIA PREININGER*, URSULA SAUER, STEFAN OBERSRIEBNIG and MAX TROMBITAS

ARC Seibersdorf Research GmbH, Department of Bioresources, 2444 Seibersdorf, Austria

(*Received 5 November 2004; in final form 12 January 2005*)

3D-materials, such as cross-linked poly(vinyl alcohol) (PVA), PVA/monochlorotriazinyl-β-cyclodextrin (MCT)-doped sol-gel and modified melamine particles were employed as an immobilization matrix for proteins in order to obtain enhanced signal-to-noise ratios. Cross-linking PVA surfaces with cyanuric chloride (TsT) leads to 1.4-fold signal enhancement, whereas linking with MCT results in five times stronger signals. Signals obtained from PVA/MCT-doped sol-gel materials were up to eight times stronger, since MCT contributed to improved interconnection of the sol-gel and covalent binding of IgG. Moreover, 1.1 μm melamine particles derivatized with TsT or MCT or with no crosslinker were used for immobilization of proteins. The particles were arrayed onto the chip in various buffer or hydrogel solutions. The best results were achieved for melamine particles in PEG and PVA solutions containing MCT as a crosslinker.

Keywords: Protein chip; Microarray; Hydrogel; Poly(vinyl alcohol); Microparticle

1. Introduction

In biochip-based analytical systems, the critical factor influencing robustness and detection thresholds is the signal-to-noise ratio. Most biochips suffer from the disadvantage of insufficient signal-to-noise ratios, and thus they may only utilize molecules of medium to high abundance. In order to enhance the strength of the signal, for example in identifying regulatory proteins, different strategies are followed: (a) the development of 3D surfaces (hydrogels) and multifunctional structures (dendrimers, grafted polymers) [1, 2]; (b) the use of microparticles as an immobilization matrix (polystyrene) [3, 4]; (c) employing alternative labels (metal particles, quantum dots) [5]; (d) optimizing chip-processing parameters [6–8]; and (e) the use of more sensitive detection techniques (evanescent wave technology) [9].

*Corresponding author. Fax: +43-50550-3666. Email: Claudia.preininger@arcs.ac.at

International Journal of Environmental Analytical Chemistry
ISSN 0306-7319 print: ISSN 1029-0397 online © 2005 Taylor & Francis
DOI: 10.1080/03067310500154775

In this article we focus on hydrogels and microparticles for the purpose of antibody immobilization.

Proteins are chemically and physically heterogeneous, are known to become less active when bound to a solid surface and most adsorb non-specifically to commonly used substrate materials. Hence, the performance of protein chips as well as their specificity and sensitivity are limited when used in diagnostic devices. As a consequence, materials such as hydrogels, providing a three-dimensional, solution-like environment, are used in order to keep the protein spots hydrated at all times and to prevent the proteins from denaturing. In this respect, humidity control during arraying is also a crucial parameter [6]. The hydrogel surfaces reported in literature are based on polyacrylamide [10], poly(ethylene glycol) [11] and agarose [12, 13]. The main advantages of hydrogels are hydrophilicity, low non-specific binding and high loading capacity. However, hydrogels often have the disadvantages of low mechanical stability and long processing times due to thicker layers and increased diffusion limits. The preparation of some hydrogels, for instance polyacrylamide, is particularly time-consuming.

In the following, we report on mechanically stable poly(vinyl alcohol) (PVA) surfaces achieved by either cross-linking with cyanuric chloride (TsT) or monochlorotriazinyl-β-cyclodextrin (MCT) or by doping sol-gel with poly(vinyl alcohol). The latter matrix combines the mechanical stability of silanes with the hydrophilicity and biocompatibility of the hydrogel. The use of hydrogel-doped sol-gels in optochemical (bio-) sensors has been described, with polydimethylsiloxane [14], poly(vinyl alcohol) [15], chitosan [16] and hydroxyethyl carboxymethyl cellulose [17] being used as dopants. To our knowledge, we have been the first to use hydrogel-doped sol-gels as an immobilization matrix in protein chips. To date, sol-gel has been used in sol-gel/antibody solutions for pin spotting protein arrays [18, 19]. N. Rupcich *et al*. [19] demonstrated that, compared with conventional aldehyde slides, the arraying of antibody/sol-gel solutions results in 106-times brighter arrays and 40-fold higher signal-to-noise ratios.

Microparticles can also be used as three-dimensional immobilization matrices. Such immobilized particle arrays offer a format allowing higher signal-to-noise ratios due to higher-density multiplexing and a greater scattering coefficient. In most cases, (modified) polystyrene- and poly(ethylene glycol) (PEG) particles are employed [3, 4]. In the present study, melamine particles were coupled to IgG using cyanuric chloride (TsT) or monochlorotriazinyl-β-cyclodextrin (MCT) and arrayed in buffer or hydrogel onto various chip surfaces.

The 3D-matrices reported herein were evaluated with respect to signal-to-noise ratio and fluorescence background using IgG and Dy633-labelled anti-rabbit IgG as probe and target in a direct immunoassay.

2. Experimental

2.1 *Materials*

Glass slides (25×75 mm) (No. 58902), Silane-Prep^{TM} slides (25×75 mm) (No. S4651) and tetraethoxysilane (TEOS) were purchased from Sigma. Chloroform and Tween-20 were obtained from Fluka, 3-aminopropyltriethoxysilane from Gelest. Dodecyl sulfate sodium salt (SDS) was purchased from Merck and phosphate buffered saline (PBS) from Gibco. $20 \times$ saline-sodium citrate (SSC) Ultra Pure^{TM} was obtained from

Invitrogen, while 10 × PBS originated from Gibco, β-cyclodextrin (β-CD) and Cavasol® W7 MCT (monochlortriazinyl-beta-cyclodextrin Na-salt) from Wacker and cyanuric chloride (TsT) from Aldrich.

2.2 *Chip surfaces*

Unless otherwise indicated, all chip surfaces were prepared using a commercial coating device (Erichsen, model 360). The wet-layer thickness was 15 μm. Typically 2 days after preparation, hydrogel-doped sol-gel slides were coated onto Silane Prep™ slides from the cocktails listed in table 1, subsequently dried at 37°C and stored at room temperature until use.

Poly(vinyl alcohol) (PVA) slides were cast from solutions of 0.5% PVA in DMSO and dried overnight in the hood.

PVA/MCT slides were prepared according to [20]. Briefly, the slides were incubated in a solution of 10% MCT (pH 10) for 1 h and dried at room temperature. MCT was thermally fixed on PVA at 150°C for 10 min, then washed thoroughly and dried at room temperature.

PVA/cyanuric chloride (TsT) slides were prepared as described at www.pall.ca/OEM_4765.asp. Briefly, the slides were immersed in triethylamine/CH_2Cl_2 for 2 min and, after the addition of TsT, incubated under gentle agitation for 1 h. The slides were subsequently washed in CH_2Cl_2 and blow-dried using compressed air. PST-*co*-VBT slides were prepared by coating Silane Prep™ slides with poly(styrene-*co*-4-vinylbenzyl thiocyanate) (1 vol.% in chloroform) [21]. The chip was dried at room temperature without additional curing and pre-activated at 450 mJ cm^{-2} in a UV Stratalinker™ 2400 (Stratagene) before spotting.

Agarose slides were prepared by dip-coating aldehyde slides in a 1% agarose solution. For improved adhesion, the glass slides were dipped in the hydrogel solution twice. The slides were dried and activated using 20 mM $NaIO_4$ for 30 min before spotting.

Aldehyde and nitrocellulose slides were purchased from Telechem and Schleicher & Schuell respectively.

2.3 *Activation of melamine particles*

A solution of 10% 1.1 μm melamine particles in H_2O was obtained from Microparticles GmbH (Germany). Particle solution (1 mL) was used for derivatization with either MCT or TsT according to the procedures described above.

Table 1. Composition of sol-gel cocktails. Relative fluorescence (a.u.) (flu) and percent fluorescence background (BG) of PVA and PVA/MCT-doped sol-gel, agarose, PST-*co*-VBT, aldehyde and nitrocellulose surfaces.

Surface	TEOS	EtOH	PVA	PVA : MCT 1 : 2	PVA : MCT 1 : 1	PVA : MCT 2 : 1	flu (a.u.)	% BG
Sol-gel 0	1	2	3	–	–	–	1184	55.5
Sol-gel 1 : 2	1	2	–	3	–	–	1447	25.0
Sol-gel 1 : 1	1	2	–	–	3	–	3404	23.0
Sol-gel 2 : 1	1	2	–	–	–	3	9361	6.6
Agarose	–	–	–	–	–	–	281	77.6
PST-*co*-VBT	–	–	–	–	–	–	7332	11.4
Aldehyde	–	–	–	–	–	–	1180	62.7
Nitrocellulose	–	–	–	–	–	–	13647	3.2

2.4 *Coupling of IgG to melamine particles*

Dry melamine (0.5 mg), melamine/MCT and melamine/TsT particles were incubated in 1 mg mL^{-1} Dy633-labelled anti-rabbit IgG in 0.1 N carbonate buffer (pH 9) under vigorous shaking overnight. After coupling, the particles were filtered and taken up in 1 mL PBS (pH 7.2) resulting in a 2% particle solution, which was diluted with the printing buffer (see table 2) in a ratio 1 : 1.

2.5 *Arraying*

Solutions (0.6 nL) of 0.1–0.5 mg mL^{-1} rabbit IgG (Sigma, I8140) in H_2O, 3 × SSC/1.5 betaine/0.01% SDS, 0.1 N phosphate buffer (pH 8)/10% glycerin, 0.1 N phosphate butter (pH 8)/0.01% SDS and PBS (pH 7.2) were printed in triplicate on PVA and sol-gel slides using the OmniGrid^{TM} contact spotter by GeneMachines (pin SMP3). The print buffers used for the particle arrays are presented in table 2 (final concentrations). Particles P1 to P3 stand for Dy633-labelled anti-rabbit IgG immobilized on particles which were derivatized with TsT, MCT (pH 9) and MCT (pH 10) respectively. After arraying, all slides were left overnight at 40% humidity on the slide holders of the arrayer.

2.6 *Blocking*

For surface blocking, slides were immersed in PBS (pH 7.2)/0.1% Tween-20 for 1 h, subsequently washed in PBS and blow-dried with compressed air.

Table 2. Composition of print buffers 1 to 25 used in particle arrays.

No.	Composition
1	6 × SSC, 3 M betaine
2	0.1 M carbonate buffer (pH 9.6)
3	0.1 M carbonate buffer (pH 9.6), 0.02% SDS
4	0.1 M carbonate buffer (pH 9.6), 2% glycerin
5	0.1 M carbonate buffer (pH 9.6), 20% glycerin
6	0.1 M carbonate buffer (pH 9.6), 2% trehalose
7	0.1 M carbonate buffer (pH 9.6), 20% trehalose
8	2% PVA in H_2O/DMSO
9	10% PVA in H_2O/DMSO
10	2% PVA in H_2O, 0.02% SDS
11	2% PVA in H_2O
12	2% PVA, 6 × SSC, 3 M betaine, 0.02% SDS
13	2% PVA in carbonate buffer (pH 10.2), 0.02% MCT, DMSO
14	2% PVA in carbonate buffer (pH 10.2), 0.2% MCT, DMSO
15	4% PEG35000, 1% MCT in H_2O
16	0.4% PEG35000, 0.1% MCT in H_2O
17	0.4% PEG35000 in H_2O
18	0.4% Pluronic 2035, 0.1% ßCD in H_2O
19	0.4% Pluronic 6800, 0.1% ßCD in H_2O
20	0.4% Pluronic 8100, 0.1% ßCD in H_2O
21	0.4% Pluronic 10500, 0.1% ßCD in H_2O
22	4% PEG35000, 1% ßCD in H_2O
23	0.4% PEG35000, 0.1% ßCD in H_2O
24	0.1 M carbonate buffer (pH 9.6), 2% ethyleneglycol
25	0.1 M carbonate buffer (pH 9.6), 20% ethyleneglycol

2.7 *Direct immunoassay and read-out*

The immobilized IgG probes were processed with 4 ng μL^{-1} Dy633-labelled anti-rabbit IgG in PBS (pH 7.2)/0.1% Tween-20 at 4°C for 3 h, washed in PBS (pH 7.2) and blow-dried with compressed air. Detection and signal processing of the array was carried out using a Genepix^{TM} 4000B non-confocal scanner from Axon Instruments along with the corresponding software.

3. Results and discussion

3D-materials, such as cross-linked poly(vinyl alcohol) (PVA), PVA/monochlorotriazinyl-β-cyclodextrin (MCT)-doped sol-gel and modified melamine particles were evaluated as immobilization matrix for proteins. Improved immobilization capacity and mechanical stability due to cross-linking and copolymerization are reported. The effect of printing buffers on the signal intensity is discussed.

3.1 *Cross-linked poly(vinyl alcohol) (PVA): MCT* vs. *TsT*

Poly(vinyl alcohol) surfaces were cross-linked with cyanuric chloride (TsT) or monochlorotriazinyl-β-cyclodextrin (MCT) as described in section 2.1. Compared with plain PVA surfaces, PVA/TsT surfaces resulted in 1.4-fold signal enhancement, PVA/MCT in 4.8-fold enhancement. The signal enhancement is most likely due to the increased mechanical stability of the hydrogel and the covalent linkage of IgG molecules on the derivatized surfaces. Figure 1 shows the fluorescence signal (a.u.) of 0.5 mg mL^{-1} IgG in H_2O, PBS (pH 7.2), 3 × SSC/1.5 M betaine/0.01% SDS, 0.1 N phosphate buffer (pH 8)/10% glycerin and 0.1 N phosphate buffer (pH 8)/0.01% SDS. It may be plainly seen that signal intensity depends on the choice of print buffer. Except for IgG in 3 × SSC/1.5 M betaine/0.01% SDS, the signals are clearly enhanced on PVA/MCT surfaces. The greatest fluorescence, 2.6 to 4-fold greater than on PVA/TsT surfaces, was obtained for IgG in H_2O and in 0.1 N phosphate buffer (pH 8)/0.01% SDS respectively. The greatest difference in signal intensity was measured for IgG in PBS (pH 7.2): a 6.4 times stronger signal was observed

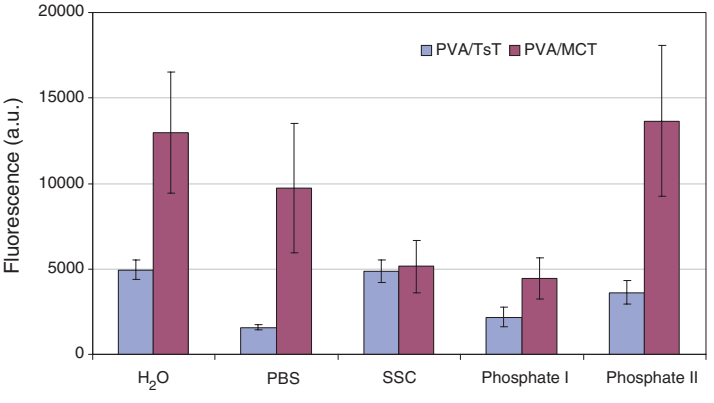

Figure 1. Relative fluorescence (a.u.) of processed IgG in H_2O, PBS, SSC/betaine and phosphate buffers I and II using TsT- and MCT-modified PVA-surfaces.

on PVA/MCT as compared with PVA/TsT surfaces. A possible explanation for the more intense signals might be the large size of the cross-linker. MCT is a bulky molecule with an average molecular weight of 1560, while TsT in contrast is a small compact molecule with a molecular weight of 184.41. The larger cross-linker provides for a greater distance between immobilized IgG and the surface and thus a lower density of immobilized IgG molecules. Hence, the IgG molecules are lifted farther away from the surface and become more easily accessible for the target.

3.2 *PVA/MCT-doped sol-gel*

Cross-linked PVA-silica gels were prepared according to table 1, and their performance was compared to agarose, PST-*co*-VBT, aldehyde and nitrocellulose surfaces. Sol-gel was doped with PVA/MCT and employed at ratios of 1 : 2, 1 : 1 and 2 : 1. As evident from the fluorescence data in table 1, IgG on PVA/MCT (2 : 1)-doped sol-gel resulted in eight-fold signal enhancement as compared with plain PVA-doped sol-gel. In general, the signal increased with an increased amount of PVA cross-linked with MCT. PVA/MCT obviously leads to improved cross-linking of the hydroxy groups of PVA and silica (equation (5)) as a result of the polycondensation reactions. Furthermore, the IgG molecules might not only be entrapped in the PVA-doped sol-gel pores, which in contrast to those resulting from acidic catalyzation are sufficiently large, but also bound to the surface by means of the dopant MCT (MCT contains 2–3 reactive groups per molecule). Thus, MCT can serve as a cross-linker both for PVA (equation (6)) and between the IgG and the chip surface. Cross-linking agents also increase gel flexibility and reduce shrinkage during the drying and aging process while at the same time improving the homogeneity of the silica sol-gel and providing crack-free surface layers. Moreover, background is reduced drastically with the addition of MCT. The signal-to-noise ratios for PVA-, PVA/MCT (1 : 2)-, PVA/MCT (1 : 1)- and PVA/MCT (2 : 1)-doped sol-gels are 1.8, 4.0, 4.3 and 15.2, respectively, indicating significantly enhanced sensitivity on MCT-cross-linked PVA-doped sol-gels (see figure 2). Signal enhancement may probably also be attributed

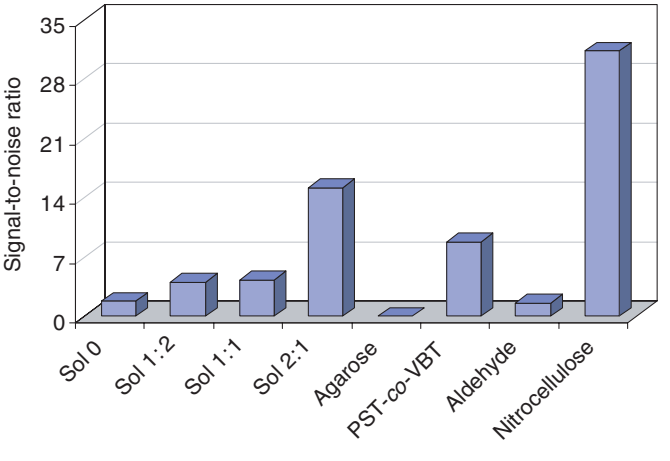

Figure 2. Signal-to-noise ratios of IgG, processed with Dy633-labelled anti-rabbit IgG on sol-gel 0, 1 : 2, 1 : 1 and 2 : 1, agarose, PST-*co*-VBT, aldehyde and nitrocellulose surfaces.

to stronger interconnection within the sol-gel network, as the dopants are not only physically entrapped but also covalently linked (equations (5) and (6)). Stronger linkage also leads to a more rigid surface which is less prone to inter- and intra-array variations. (Ph. Angenendt *et al.* [2] compared gel-coated and non-gel-coated chip surfaces and found greater signal variations for antibody arrays on gel-coated chips. This might be due to the material being soft and swellable.)

Apart from the dopant, other parameters, such as temperature, pH and relative concentrations of silica precursor, EtOH and water, also affect hydrolysis and polycondensation reactions. Under an alkaline pH (pH 10), the condensation process is rapid and hydrolysis slow. Possible hydrolysis and condensation reactions are listed in equations (1–6):

$$Si(OEt)_4 + H_2O \rightarrow (EtO)_3Si-OH + EtOH \quad (1)$$

$$HO-Si(EtO)_3 + H_2O \rightarrow (EtO)_2Si(OH)_2 + EtOH \quad (2)$$

$$(EtO)_3Si-OH + (EtO)_4Si \rightarrow (EtO)_4Si \rightarrow (EtO)_3Si-O-Si(OEt)_3 + EtOH \quad (3)$$

$$(EtO)_3Si-OH + HO-Si(OEt)_3 \rightarrow (EtO)_3Si-O-Si(OEt)_3 + H_2O \quad (4)$$

$$(-CH_2-\underset{\displaystyle OH}{\underset{|}{CH}}-)_x + (EtO)_4Si \rightarrow -CH_2-CH-O-Si(OEt)_3 + EtOH \quad (5)$$

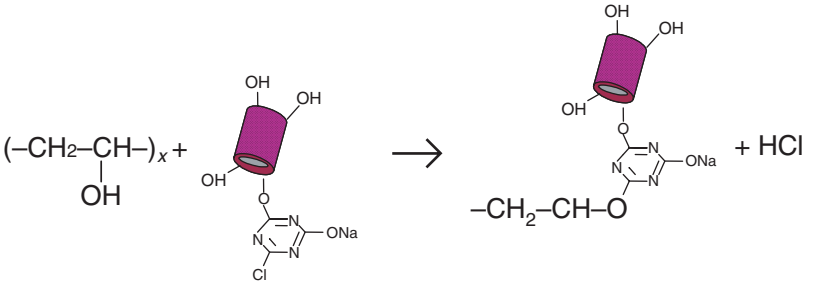

(6)

The equations lead one to expect a well-interconnected pore network. Due to the condensation reactions and the evaporation of EtOH during coating, the sol-gel layer becomes enriched with water and thus precisely meets certain requirements for protein chip surfaces, such as that of providing a quasi-liquid environment.

Compared with agarose and aldehyde slides, the PVA/MCT (2 : 1) doped sol-gel slides were clearly superior, with the signal being eight times stronger, and compared with PST-*co*-VBT the results were increased by 20%. However, nitrocellulose slides displayed the best performance (one-third better signal and two times greater signal-to-noise ratio).

3.3 *Melamine particles*

Dy633-labelled IgG/melamine particles P1 to P3 were printed in buffer and hydrogel solutions onto PVA surfaces in order to evaluate the most appropriate print buffer for the particle array.

The choice of print buffer is critical for the signal intensity, spot homogeneity and protein activity. Reagents such as glycerin and trehalose are added to stabilize protein activity, while additives such as DMSO are applied to slow down solvent evaporation and thus create more homogeneous spots. By way of alternative to aqueous buffers, hydrogels can be used to increase immobilization capacity as they form a three-dimensional particle spot on the surface.

The printing solutions tested contained various concentrations of detergents, polysaccharides, hydrogels, cross-linking agents and organic solvents. A detailed description is given in table 2. The print buffers highlighted in bold letters led to the best results. No fluorescence signals were observed in the other buffers tested, an observation most likely to be attributed to particles settling in the microtiter plate during arraying. Figure 3 shows the fluorescence signal of fluorescent particles in printing solutions 10, 13–16, 18, 22, 24 and 25 at various intervals, specifically 0, 1, 2 and 3 h after vigorous shaking and the beginning of the printing process. Figure 4 shows the respective fluorescence images. As is obvious from figure 3, signal intensity drops with time as the particles settle in the microtiter well and particle concentration is altered. This is most evident from buffers 10 and 24. Printing solutions of polymers such as PVA (buffers 13 and 14), with a high molecular weight, resulted in a 50–60% decrease within the first hour, whereas afterward the concentration remained constant. The strongest signals by far were achieved in using buffers 13 and 14. When the results from these buffers are compared to the other PVA buffers tested, it becomes obvious that the type as well as the concentration of the additive play a crucial role in signal strengths: too high hydrogel concentrations in the printing buffer retard the diffusion of the target to the immobilized particle spot, thus causing weaker signals; too low buffer concentrations lack sufficient viscosity and have almost no stabilizing effect on the protein. Furthermore, particles in low-viscosity buffers may settle in the microtiter plate during arraying and hence alter particle concentration. Cross-linking agents, such as MCT, can strengthen the hydrogel network, rendering the hydrogel more stable

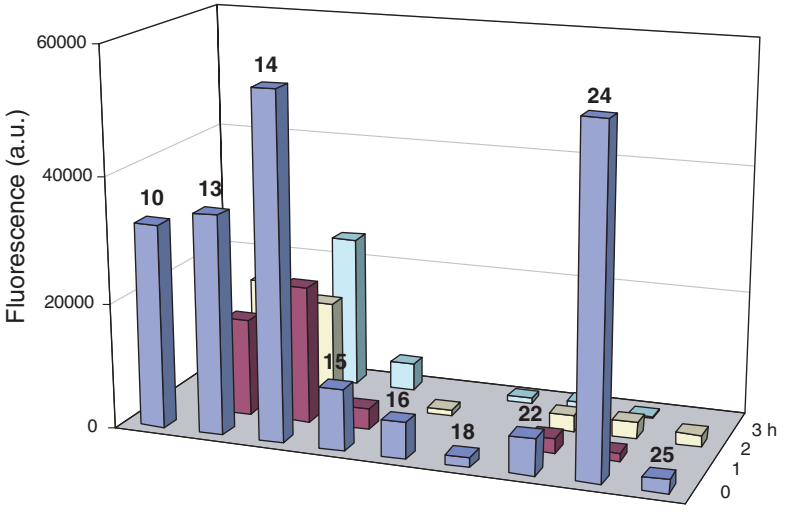

Figure 3. Fluorescence signals of Dy633-labelled antibody in print buffers 10, 13–16, 18, 22, 24 and 25, when arrayed onto the chip in hourly intervals.

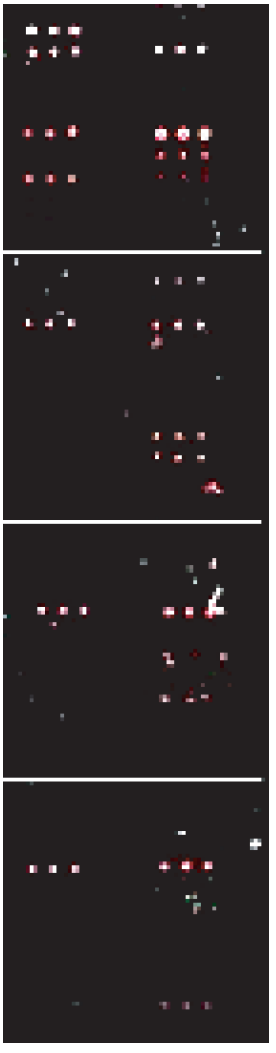

Figure 4. Fluorescence images of particle spots arrayed onto PVA surfaces at time 0, and after 1, 2 and 3 h (from above).

in mechanical terms, and furthermore covalently bond the hydrogel spot to the surface. The addition of DMSO results in more compact spots while carbonate buffer (pH 10.2) facilitates the cross-linking reaction. In contrast, high salt-PVA solutions (no. 12) lead to precipitation.

Buffers 15, 16 and 22 were derived from injectable drug delivery systems that make use of cyclodextrin-PEG based gels to increase the interaction between protein molecules [22].

Both PVA and PEG are polyhydroxy compounds that act as volume expanders, increasing the water density around the protein by forming hydrogen bonds, and hence they can support the activity and stability of the protein.

Compared to immobilized 0.1 mg mL^{-1} Dy633-labelled IgG the particle spots resulted in two times enhanced signals in buffer 15, and 5 to 10 times enhanced

signals in buffer 13 and 14, depending on what kind of chip surface was used as immobilization matrix. Future work will aim at further optimization of the print buffer and immobilization chemistry, and the application of particle arrays in environmental diagnostics.

References

[1] P. Peluso, D.S. Wilson, D. Do, H. Tran, M. Venkatasubbaiah, D. Quincy, B. Heidecker, K. Poindexter, N. Tolani, M. Phelan, K. Witte, L.S. Jung, P. Wagner, St. Nock. *Anal. Biochem.*, **312**, 113 (2003).
[2] P. Angenendt, J. Glökler, D. Murphy, H. Lehrach, D.J. Cahill. *Anal. Biochem.*, **309**, 253 (2002).
[3] P.W. Stevens, C.H.J. Wang, D.M. Kelso. *Anal. Chem.*, **75**, 1141 (2003).
[4] C. Tozzi, A. Salomone, G. Giraudi, L. Anfossi, C. Baggiani, C. Giovannoli. *Anal. Chim. Acta*, **510**, 153 (2004).
[5] W. Fritzsche, T.A. Taton. *Nanotechnology*, **14**, R63 (2003).
[6] C. Preininger, U. Sauer, J. Dayteg, R. Pichler. *Bioelectrochem.*, **67** (2005), in press.
[7] M.K. McQuain, K. Seale, J. Peck, S. Levy, F.R. Haselton. *Anal. Biochem.*, **320**, 281 (2003).
[8] Ch.-S. Lee, B.-G. Kim. *Biotechnol. Lett.*, **24**, 839 (2002).
[9] P. Bao, A.G. Frutos, C. Greef, J. Lahiri, U. Mueller, T.C. Peterson, L. Warden, X. Xie. *Anal. Chem.*, **74**, 1792 (2002).
[10] A.Y. Rubina, E.I. Dementieva, A.A. Stomakhin, E.L. Darii, S.V. Pan'kov, V.E. Barsky, S.M. Ivanov, E.V. Konovalova, A.D. Mirzabekov. *Biotechniques*, **34**, 1008 (2003).
[11] T. Cha, A. Guo, Y. Jun, D.Q. Pei, X.-Y. Zhu. *Proteomics*, **4**, 2519 (2004).
[12] V. Afanassiev, V. Hanemann, St. Wölfl. *Nucleic Acids Res.*, **28**, 66 (2000).
[13] Y. Wei, G. Ning, Z. Hai-Qian, W. Jian-Guo, W. Yi-Hong, K.-D. Wesche. *Sensors & Act. B*, **98**, 83 (2004).
[14] D.A. Nivens, Y. Zhang, S.M. Angel. *Anal. Chim. Acta*, **376**, 235 (1998).
[15] M. Cajlakovic, A. Lobnik, T. Werner. *Anal. Chim. Acta*, **455**, 207 (2002).
[16] G. Wang, J.-J. Xu, H.-Y. Chen, Z.-H. Lu. *Biosensors & Bioelectronics*, **18**, 335 (2003).
[17] X.J. Wu, M.M.F. Choi. *Anal. Chim. Acta*, **514**, 219 (2004).
[18] E.J. Cho, Z. Tao, E.C. Tehan, F.V. Bright. *Anal. Chem.*, **74**, 6177 (2002).
[19] N. Rupcich, A. Goldstein, J.D. Brennan. *Chem. Mater.*, **15**, 1803 (2003).
[20] U. Denter, E. Schollmeyer. *J. Inclusion Phenomena. Mol. Recogn. Chem.*, **25**, 197 (1996).
[21] C. Preininger, U. Sauer, W. Kern. *Anal. Chem.*, **76**, 6130 (2004).
[22] US Patent 20020019369.